Pergamon

Int. J. Heat Mass Transfer. Vol. 40, No. 5, pp. 1227–1241, 1997

0017–9310/97 $17.00+0.00

PII: S0017–9310(96)00140–8

A physico-mathematical model of rocket exhaust plumes

E. I. VITKIN, V. G. KARELIN, A. A. KIRILLOV, A. S. SUPRUN and JU. V. KHADYKA

Institute of Physics of the Belarus Academy of Sciences, Minsk 220072, Belarus

(*Received* 31 *August* 1994)

Abstract—An axisymmetric nonisobaric supersonic jet mixing with the atmosphere or expanding into a vacuum is considered as a model of a rocket engine plume. The expanding caused by the nonisobarity, turbulent mixing and afterburning are main processes forming a plume structure at different altitudes. Optical characteristics of the plume are determined by thermal radiation of condense-phase particles and vibration–rotation transitions in molecules. In the visible and ultraviolet spectral ranges chemiluminescent mechanisms make significant contribution to plume radiation. The Navier–Stokes equations with additional terms describing chemical kinetics and vibrational relaxation have been used for numerical simulation of plumes. An original technique has been developed to calculate selective radiation transfer in nonuniform nonequilibrium medium. Calculated plume spectra of typical liquid and solid fuel rocket engines at different altitudes are presented for infrared, visible and ultraviolet ranges. Copyright © 1996 Elsevier Science Ltd.

INTRODUCTION

An exhaust plume of a rocket engine (RE) is created by interaction between its jet of exhaust products and the atmosphere and produces powerful radiation over the ultraviolet (u.v.), visible and infrared (i.r.) spectral ranges. A model of the plume describing basic physico-chemical processes which determine plume radiation over the spectral range of 0.2–10 μm is proposed in this paper. The final stage in calculating optical parameters of the plume (spectral radiant intensity and spectral radiance) includes, as a rule, integrating a radiation transfer equation over a nonuniform path running through a volume containing exhaust products and extending up to a radiation sensor. To perform the integration one should know distributions of thermodynamic parameters of the exhaust products and the atmosphere along a path of flight. It is possible to calculate the temperature and concentration of flowfields of combustion products by solving a gasdynamic problem of a supersonic two-phase jet expanding into a moving airstream, taking into account physico-chemical transformations caused by afterburning of fuel-rich exhaust products, velocity and temperature 'sliding' of condensed-phase particles relative to gas molecules and vibration relaxation of molecular gases. Therefore, creating a mathematical model of plume radiation properties implies solving problems of the following three types: gasdynamic, physico-chemical and optical.

GASDYNAMIC STRUCTURE OF THE PLUME

Basic assumption

At the flight altitudes of the first stages, the rocket plume is a supersonic turbulent jet expanding into a moving airstream. In this connection two basic assumptions of the plume theory, quasi-stationarity and axial symmetry, are quite reliable. Quasi-stationary implies that for each flight altitude the rocket plume can be considered as a steady-state jet flow with constant boundary conditions. Also, it means that the coordinate system used for calculations is rigidly bound to an airframe. Since the rocket accelerates (the airstream velocity diminishes downstream from a nozzle exit) so the assumption made can lead to errors if one calculates plume properties for distances exceeding several thousands of nozzle exit radii downstream. In reality, however, this restriction is not important because the centerline exhaust temperature (and plume radiance) decreases much more significantly than the airstream velocity does. In other words, the radiation size of a typical first stage RE plume is many times less than the distance scale (measured along a flight trajectory) along which the rocket velocity does not substantially change.

The 'equivalent nozzle' assumption, which reduces the plume to an axisymmetric one, not only enables one to simplify calculations greatly, but also excludes many variables describing details of a rocket construction. The assumption is based upon experiments in wind tunnels and does not produce large errors if one does not calculate radiance of a nearfield zone close to the nozzle exit because beyond bounds of the nearfield shock structure, spatial distributions of gasdynamic variables of a composite jet are slightly different from the distributions of a single jet and because afterburning processes develop just within a pressure-equilibrated farfield of the plume.

In general, a gasdynamic structure of the plume is divided into two zones: nearfield shock structure and

NOMENCLATURE

A_ν	source function
$A_{\nu\,own}$	own condensed-phase radiation coefficient
$B_k(\nu)$	extension of the Plank function to nonequilibrium conditions
B_ν	rotational constant
C_i	weight fraction of the ith gas species
F_{pk}	empirical coefficients determining the rate of momentum exchange between gas and particles
H	total specific enthalpy
I_ν	spectral radiance
I_{ext}	external radiance
J_λ	emission coefficient
K_ν	attenuation coefficient
$k_{\nu\,gas}$	gas-phase absorption coefficient
$k_{\nu\,abs}$	absorption coefficients of the condensed phase
$k_{\nu\,scat}$	scattering coefficients of the condensed phase
M	Mach number
P	gas pressure
$p(\cos\Theta)$	phase function
Pr	Prandtl number
q	gas speed
q_{ks}	tangent velocity of the condensed phase
q_{kn}	normal velocity of the condensed phase
$q_{\nu'\nu}$	Frank–Condon factor
R	radius
S_e	square of the matrix element of the molecular dipole momentum
T	temperature
T_k^*	temperature of a gas braking on a particle
T_r	rotational temperature of the upper electron state [K]
u	axial velocity
v	radial velocity
W	specific radiation power of the gas component
W_k	specific radiation power kth particle class
x, r	coordinates of the cylindrical system.

Greek symbols

ε_α	number of vibrational quanta
ζ_i	production rate of the ith species in chemical reactions
θ	angle between the tangent of the streamline and the symmetry axis
Θ	scattering angle
κ	coefficient of turbulent viscosity
μ_i	molecular weight
ρ	density
τ	transmissivity
Φ_{pk}	empirical coefficients determining the rate of heat exchange between gas and particles
ψ	Mises coordinate for gas
ψ_k	Mises coordinate for the kth class of particles.

Subscripts

a	conditions at the nozzle exit plane
i	ith gas species
k	kth class of particles.

pressure-equilibrated farfield. A gaseous jet flowing out of a supersonic nozzle and having its static pressure different from that of the surrounding atmosphere (under- or overexpanded jet) produces a complicated periodic structure of shock and expansion waves. Downstream of a series of pulsations (barrel shocks) the axial static pressure equalizes the ambient pressure at the isobaric section of the plume and the pressure-equilibrated farfield begins. In some models the nearfield shock structure adjoins the nozzle and is characterized by sharp nonuniformity of gasdynamic flowfield patterns and shock waves are neglected because the contribution of the pressure-equilibrated farfield to the overall plume radiant intensity significantly exceeds the contribution of the nearfield shock structure even for liquid propellant RE having relatively low concentrations of fuel-rich exhaust products. However, retaining the structure is advantageous because it allows one to calculate radiance distributions in the nearfield and eliminate errors arising from recalculation of exit plane parameters to that of the isobaric section.

Moreover, ignition of the fuel-rich plume products begins in a mixing layer arising on the periphery of the first barrel shock and sometimes ends there if ambient pressure is too low to maintain afterburning processes in the pressure-equilibrated farfield. Inside a central zone bordered by a barrel shock, the plume gases undergo substantial expansion and cooling so effects of particle velocity and temperature 'sliding' begin to arise (particle velocity and temperature lag behind gaseous ones). Neglecting these effects means that one cannot correctly derive parameters in the beginning section of the pressure-equilibrated farfield.

Plume farfield patterns can be assessed by solving parabolized Navier–Stokes equations in which viscosity, diffusivity and thermal conductivity are determined by turbulent transfer [1]. There are many different models predicting turbulent mixing. These models contain a large number of empirical constants

Table 1. Standard chemical scheme of 10 reactions [3, 4]

$OH+H_2 = H_2O+H$
$OH+OH = H_2O+O$
$O+H_2 = OH+H$
$H+H+M = H_2+M$
$H+O+M = OH+M$
$H+OH+M = H_2O+M$
$O+O+M = O_2+M$
$CO+OH = CO_2+H$
$CO+O+M = CO_2+M$

fitted for better description of either individual problem class. In the paper the $k\varepsilon$-model of turbulent viscosity [2] is used. This model enables one to describe mixing over a wide range of flow parameters.

Chemical kinetics

The most important mechanism determining plume radiation at low altitudes is afterburning that is initiated by mixing exhaust products (usually, they contain CO and H_2) with the atmosphere. In this case, a proper selection of the afterburning mechanism is an important element of plume flowfield calculations. The standard chemical scheme [3, 4] containing 10 gas-phase reactions is commonly used (Table 1).

The scheme enables one to predict basic regularities of temperature and species concentration behavior in the plume. However, attempts have been made to add reactions of chlorine-containing species to the scheme (because a solid propellant RE exhaust includes a significant concentration of HCl), reactions of H_2O [5] (which enable one to more precisely calculate temperature and species patterns in peripheral low-temperature zones of the plume), reactions of nitrogen-containing species [6] (to improve description of plume ignition at low pressures, which is an important factor if ambient pressure substantially changes as the rocket follows its trajectory) etc.

A detailed study of chemical kinetics for plume-specific conditions enabled us to deduce several basic regularities. Characteristic times of bimolecular (exchange) and termolecular (recombination) reactions differ by several orders of magnitude. A mixing time, the third characteristic time of the afterburning plume, is determined by the rate of air penetration into the plume. Reciprocal times of these processes (U_{mix}, U_{exc}, U_{rec}) as approximate functions of plume variables can be represented as follows:

$$U_{\text{mix}} \simeq \eta_t/R^2; \quad U_{\text{exc}} \simeq \rho D_2 \exp(-E/T)y;$$

$$U_{\text{rec}} \simeq \rho^2 D_3 y^2$$

where η_t is eddy viscosity; ρ, R, U, T, y are typical plume density, radius, axial velocity, temperature, and radical species concentration, respectively. During the initial stage of afterburning, when there is lack of oxygen in the plume, decreasing of radical concentrations due to turbulent mixing competes with radical production in bimolecular reactions. Until the following condition

$$\eta_t > \rho R^2 D_2 \exp(-E/T) \tag{1}$$

is valid the radical concentrations are so small that there is no afterburning. Parameters D_2 and D_3 depend on plume composition and E is activation energy of a typical exchange reaction.

When the condition in system (1) is violated the number of active radicals in the plume increases exponentially. Rates of bimolecular reactions become so high that in the whole afterburning farfield they are in equilibrium, this means that the number of radicals depend on plume composition and temperature rather than the reaction rates. Termolecular recombination reactions are of great importance in this stage, only these reactions reduce the number of gas molecules and produce heat. Now the mass conservation equation for a species can be written in the form:

$$\partial y/\partial x = -L(y)+S \tag{2}$$

where $L(y) \simeq \mu_t y$ is a mixing operator (μ_t is a constant coefficient) and $S \simeq (R/U)\rho^2 \Sigma D_{ik} y_i y_k$ determines species removal in termolecular reactions (D_{ik} are reaction rates). Combustion behavior is determined by the ratio of these two terms. At low altitudes (ambient pressure is relatively high) the condition $S \gg L(y)$ is valid. This causes the amount of products burnt and heat production to be only governed by the rate with which oxygen mixes with the plume. The mode of plume afterburning takes place at altitudes of 10–15 km. As heat generation depends upon pressure quadratically so S rapidly decreases with altitude. The plume enters the mode in which concentration profiles are formed by mixing rather than afterburning. Finally rates of termolecular reactions become so low that heat production due to afterburning can no longer compete with cooling caused by air penetrating the plume due to mixing. The plume temperature drops drastically and afterburning stops. The altitude at which afterburning stops depends on the following parameters: the equivalent nozzle diameter, and nozzle and isobaric section temperatures. The second temperature in turn depends upon the exit pressure. Plumes of real rocket engines stop to afterburn at altitudes of 30–50 km—the lighter the rocket, the lower this altitude. The first stages are separated in the same altitude range.

In broad outline there is a mechanism of interaction between chemical kinetics and gasdynamic processes in plumes. A knowledge of the afterburning mechanism has been explicitly used for calculation techniques and has enabled us to simplify and considerably speed up calculations. Also, this knowledge is an analysis tool that makes it possible to investigate the influence of either a chemical reaction or its rate constant on afterburning which strongly affects plume radiation.

By developing the afterburning calculation tech-

nique the authors have created a method enabling one to flexibly modify the chemical reaction mechanism used [7]. The method comprises a minibank containing up to 100 gas phase chemical reactions and their rate and equilibrium constants and a program preprocessor that automatically creates a subroutine intended to calculate the right sides of kinetic equations for a user-selected reaction mechanism.

Particles

For solid propellant rocket engines a correct description of gas–particle interaction is of great importance in calculating gasdynamic flowfields and radiation features. In plumes there are conditions, at which on the one hand, particle–particle interaction can be neglected and on the other hand, particles considerably affect plume flowfields and radiance distributions. To obtain a mathematical description of this two-phase flow we have to add source terms to Navier–Stokes momentum and energy conservation equations and include Newton equations of motion for every particle class. Empirical functions [8] for gas–particle interaction coefficients obtained by investigating particle motion in nozzles can be used.

Condensed phase particles leaving from a nozzle can be both solid and liquid. Transferring heat to gas and losing it due to emission of radiation, liquid particles transit to the solid state at the end. A correct description of phase transitions in particles is necessary for determining the gasdynamic flowfields of gas and particles and is especially important for calculating solid phase radiation because optical properties of liquid and solid particles are extremely different.

The simplest way of describing nonequilibrium crystallization of Al_2O_3 particles in RE jets is a 'recalescence' technique [9, 10]. It assumes that while being cooled Al_2O_3 particles stay liquid at temperatures less than the crystallization one $T_c(T_c = 2300\ \mathrm{K})$ until the recalescence temperature $T_r(T_r = 1860\ \mathrm{K})$ is reached. Then particles begin to crystallize with this process being accompanied by the instant temperature rise up to the melting point due to release of crystallization heat. In developing a calculation program we used precisely this technique.

Separation of the first rocket stage (and ignition of the second one) takes place in highly rarefied air at ambient pressures being less than 0.01 atm, also the thrust of the second stage RE is several times less than the thrust on the first one. Due to a high difference between exit plane and ambient pressures, plume products sharply cool inside the borders of the first barrel shock and their temperatures in the isobaric section turn out too low to activate afterburning. As a result, the plume radiant intensity per thrust unit drops more than ten times. The gaseous component of the plume diminishes its contribution to the plume radiation while the condensed phase increases.

A gasdynamic problem for the second rocket stage is simpler than the first stage one because chemical reactions are 'frozen' but vibrational degrees of freedom are still in equilibrium with translational ones. Therefore a simple ideal gas model can be used to calculate plume flowfields. A single nonstandard effect to be accounted for is thermal and velocity 'sliding' of condensed phase particles.

As the flight altitude rises so do dimensions of the first barrel shock. Inside the barrel shock borders, plume gases undergo abrupt cooling and accelerating followed by their heating in bow shocks with the plume pressure restoring its ambient value behind the shocks. In the near exit area of the barrel shock, where gas densities are relatively high, condensed phase particles turn apart. Under further pressure lowering along tubes of flow the particles cease to follow the gas velocity and move under their own momentum, i.e. rectilinearly. They quickly go through narrow compression zones behind bow shocks and 'stick' into the denser ambient stream. A jacket of Al_2O_3 particles arises around the plume; the particles can also be heated due to braking in the ambient stream.

Basic equations

The system of equations quantitatively describing previously mentioned processes has the following form:

$$\frac{\partial}{\partial x}(\rho u r) + \frac{\partial}{\partial r}(\rho v r) = 0,$$

$$\rho u\frac{\partial u}{\partial x} + \rho v\frac{\partial u}{\partial r} = -\frac{\partial P}{\partial x} + \frac{1}{r}\frac{\partial}{\partial r}\left(\rho\kappa r\frac{\partial u}{\partial r}\right) - \sum_k \rho_k\left(u_k\frac{\partial u_k}{\partial x} + v_k\frac{\partial u_k}{\partial r}\right)$$

$$\rho u\frac{\partial v}{\partial x} + \rho v\frac{\partial v}{\partial r} = -\frac{\partial P}{\partial r} + \frac{4}{3}\frac{1}{r}\frac{\partial}{\partial r}\left(\rho\kappa r\frac{\partial v}{\partial r}\right) - \sum_k \rho_k\left(u_k\frac{\partial v_k}{\partial x} + v_k\frac{\partial v_k}{\partial r}\right)$$

$$\rho u\frac{\partial H}{\partial x} + \rho v\frac{\partial H}{\partial r} = \frac{1}{r}\frac{\partial}{\partial r}\left(\frac{\rho}{Pr}\kappa r\frac{\partial H}{\partial r}\right) + \frac{1}{r}\frac{\partial}{\partial r}\left[\rho\kappa\frac{1-Pr}{Pr}r\frac{\partial(u^2+v^2)}{\partial r}\right] - \sum_k \rho_k\left(u_k\frac{\partial H_k}{\partial x} + v_k\frac{\partial H_k}{\partial r}\right)$$

$$\rho u\frac{\partial C_i}{\partial x} + \rho v\frac{\partial C_i}{\partial r} = \frac{1}{r}\frac{\partial}{\partial r}\left(\rho\kappa\frac{r}{Pr}\frac{\partial C_i}{\partial r}\right) + \zeta_i, \quad (i = 1, I)$$

$$\frac{\partial}{\partial x}(\rho_k u_k) + \frac{1}{r}\frac{\partial}{\partial r}(\rho_k v_k) = 0$$

$$u_k\frac{\partial u_k}{\partial x} + v_k\frac{\partial u_k}{\partial r} = F_{pk}(u - u_k)$$

$$u_k\frac{\partial u_k}{\partial x} + v_k\frac{\partial v_k}{\partial r} = F_{pk}(v - v_k)$$

$$u_k\frac{\partial H_k}{\partial x}+v_k\frac{\partial H_k}{\partial r}=\Phi_{pk}(T^*-T_k)$$
$$+F_{pk}|u_k(u-u)+v(v-v)|. \quad (3)$$

The following conventions and notations are used here: a variable without a subscript relates to a gas component; the subscript k designates the kth class of particles (they divided between the classes according to their sizes); x, r are coordinates of the cylindrical system with the axis x being directed along the stream; H is the total specific enthalpy; u and v are axial and radial velocities, respectively; C_i is the weight fraction of the ith gas species; μ_i is its molecular weight; ζ_i is the production rate of the ith species in chemical reactions; κ is the coefficient of turbulent viscosity; Pr is the Prandtl number; F_{pk} and Φ_{pk} are empirical coefficients determining the rate of momentum and heat exchange between gases and particles, T_k^* is the temperature of a gas braking on a particle:

$$T_k^*=T+|(u-u_k)^2+(v-v_k)^2|/2C_p.$$

The equation of the ideal gas state

$$\rho=P\Big/\left(RT\sum_i C_i\right),$$

concludes system (3). Temperatures of gas species and particles of each class are determined from a given enthalpy value.

The solution of system (3) is unambiguously determined by the following initial and boundary conditions:

$$u=u_a, T=T_a, C_i=C_{ia}, P=P_a,$$
$$v=0, u_k=u_{ka}, v_k=0, T_k=T_{ka}, \rho_k=\rho_{ka}$$

when $x=0$ and $r\leqslant r_a$

$$u=u_\infty, T=T_\infty, C_i=C_{i\infty}, P=P_\infty, v=0, \rho_k=0 \quad (4)$$

when $x=0$ and $r>r_a$ and when $r\to\infty$

$$\frac{\partial U}{\partial r}=\frac{\partial H}{\partial r}=\frac{\partial C_i}{\partial r}=0, \quad v=0$$

when $r=0$.

To solve the system let us introduce standardized functions (divided by their initial values) and Mises coordinates ψ for gases and ψ_k for the kth class of particles

$$\psi\frac{\partial\psi}{\partial r}=\rho ur, \quad \psi\frac{\partial\psi}{\partial x}=-\rho vr$$
$$\psi\frac{\partial\psi_k}{\partial r}=\rho_k u_k r, \quad \psi\frac{\partial\psi_k}{\partial x}=-\rho_k v_k r$$

and introduce new functions

$$\alpha=v/u, \quad \omega^2=u^2+v^2,$$
$$F_1=\sum_k\rho_k\frac{r_a}{u_a}F_{pk}, \quad F_2=\sum_k\rho_k\frac{r_a}{u_a}F_{pk}u_k;$$
$$F_3=\sum_k\rho_k\frac{r_a}{u_a}F_{pk}v_k, \quad F_4=\sum_k\rho_k\frac{r_a}{u_a}\Phi_{pk}(T_k^*-T_k),$$
$$F_5=\sum_k\rho_k\frac{r_a}{u_a}F_{pk}(u_k^2+v_k^2). \quad (5)$$

Then instead of the system (3) we can write the following:

$$\frac{\partial r}{\partial\psi}=\frac{T}{P\mu u}\frac{\psi}{r}, \quad \frac{\partial P}{\partial x}=-\gamma M^2P\frac{\Phi}{M^2-1}$$
$$\frac{\partial\omega}{\partial x}=\frac{\omega}{1+\alpha^2}\frac{\Phi}{M^2-1}+\frac{L(u)+\frac{4}{3}\alpha L(v)}{\sqrt{1+\alpha^2}}$$
$$-\frac{T}{P\mu u}\left(\omega F_1-\frac{F_2+\alpha F_3}{\sqrt{1+\alpha^2}}\right)$$
$$\frac{\partial\alpha}{\partial x}=-\frac{\phi}{M^2-1}-\frac{1}{\gamma_a M_a^2}\frac{1+\alpha^2}{u}\frac{r}{\psi}\frac{\partial P}{\partial r}$$
$$+\frac{\frac{4}{3}L(v)-\alpha L(u)}{u}+\frac{T}{P\mu u}(F_3-\alpha F_2)$$
$$\frac{\partial H}{\partial x}=\frac{1}{Pr}L(H)-\frac{T}{P\mu u}\left\{F_4+\frac{u_a^2}{T_a}\left[u\left(F_2+\alpha F_3\right)-F_5\right]\right\}$$
$$+\frac{1-Pr}{Pr}\frac{u_a^2}{T_a}L\left(\frac{\omega^2}{2}\right)$$
$$\frac{\partial C_i}{\partial x}=\frac{1}{Pr}L(C_i)+\frac{T}{P\mu u}(\rho_a u_a r_a)\zeta_i, \quad (i=1,I)$$
$$\frac{\partial r_k}{\partial x}=\alpha_k$$
$$\frac{\partial u_k}{\partial x}=F_{pk}\frac{r_a}{u_a}\frac{u-u_k}{u_k}$$
$$\frac{\partial u_k}{\partial x}=F_{pk}\frac{r_a}{u_a}\frac{v-u_k}{u_k}$$
$$\frac{\partial H_k}{\partial x}=\Phi_{pk}\frac{r_a}{u_a}\frac{T_k^*-T_k}{u_k}+F_{pk}[u-u_k+\alpha_k(v-v_k)]\frac{r_a}{u_a}\frac{u_a^2}{T_a}$$
$$\frac{\partial}{\partial\psi}\left(\frac{1}{\rho_a u_a r_a}\right)=\frac{1}{\rho_{ka}u_{ka}}\frac{1}{\psi}\frac{\partial\alpha_k}{\partial\psi} \quad (6)$$

with the notations being used in the system (6):

$$L(f)=\frac{1}{\psi}\frac{\partial}{\partial\psi}\left(\kappa\rho ur\frac{r}{\psi}\frac{\partial f}{\partial\psi}\right)$$
$$\Phi=\frac{\alpha}{r}+\frac{1}{\gamma_a M_a^2}\frac{r}{\psi}\frac{\alpha}{u}\frac{\partial P}{\partial r}+\frac{P\mu u}{T}\frac{r}{\psi}\frac{\partial\alpha}{\partial\psi}$$
$$-\frac{1}{C_pTPr}\left[L(H)-(1-Pr)\frac{u_a^2}{T_a}L\left(\frac{\omega^2}{2}\right)\right]$$

$$+\frac{M^2(\gamma-1)}{u}\left[L(u)+\frac{4}{3}\alpha L(v)\right]+\frac{1}{u}L(u)$$
$$+\sum_i\left[\frac{h_i-\int C_p\,dT}{C_p(T_a)T_a}-W_i\right]\frac{\partial C_i}{\partial x}$$
$$+\frac{F_4}{C_pP\mu u}-\frac{\gamma_a M_a^2}{P\gamma}\left\{\left[(\gamma-1)(u+\alpha v)+\frac{u}{M^2}\right]F_1\right.$$
$$\left.-\left[2(\gamma-1)+\frac{1}{M^2}\right]F_2-2\alpha(\gamma-1)F_3+\frac{(\gamma-1)}{u}F_5\right\}.$$

Equations of the above system determine solutions in the domain $0\leqslant\psi\leqslant\infty$, $0\leqslant x\leqslant\infty$. Using the transformation $z=\psi\sqrt{3+\psi^2}$ we can convert the semiaxis ψ into the unit vector interval [0, 1] with the initial jet border transforming to the midpoint of the interval. The system written is supposed to approximate real supersonic streams and it is possible to get its solution from initial conditions by the method of 'through' calculations.

FEATURES OF THE PLUME CALCULATION TECHNIQUE AT HIGH ALTITUDES

For the second rocket stage the nearfield shock structure of the RE exhaust determines optic features of the plume. This is also true for third stages and, in general, for altitudes higher than 100–150 km. There is no pressure-equilibrated farfield because dimensions of the nearfield shock structure increase sharply with altitude. Plume radiation of the third stage can be represented in the same way as the sum of the nearnozzle-zone radiation and the radiation of the zone, where exhaust products mix with the ambient stream. The mixing zone is characterized by large dimensions extending up to tens and even hundreds of kilometers and by low emission intensity comparable with that of the background. At high altitudes corresponding to third stages we can treat the nearnozzle plume zone without accounting for the influence of the ambient stream, i.e. as a jet flowing out to vacuum. The dimensions of the nearnozzle zone are essentially smaller and the radiation intensity is considerably higher than the corresponding parameters of the mixing zone. Therefore, the nearnozzle zone, as a rule, is of greatest interest at high altitudes and in this article we limit ourselves by studying the plume region only.

A feature of the third rocket stage plume is the fact that a calculation of spatial distribution of molecular species has to be performed accounting for vibrational relaxation kinetics. In turn, the kinetics has to include radiative deactivation processes. All three problems: gasdynamic, kinetic and radiative prove to be interconnected. A strict derivation of the system of equations describing the radiation transfer in vibrationally nonequilibrium gas has been given in Ref. [11]. It has been shown that under simplifying assumptions this system was equivalent to the integro-differential equation with the Biberman–Holstein source function. A numerical scheme [12] solving the equation has been also developed and problems simulating nonequilibrium jet radiation have been numerically solved. However, the RE plume radiation calculation executed by this method encounters certain difficulties due to great wastes of computational time. In this connection a simplified radiation calculation technique has been developed. With this technique the influence of the radiation on vibrational energies of molecular gases and thermal energies of condensed phase particles are considered within the bounds of the 'volume' emission approximation. This technique does not lead to noticeable errors at the spectral region, in which the plume radiation is determined by the condensed phase. As for the radiation in infrared bands of molecular gases the technique is valid for the nearnozzle plume zone (in which collisional relaxation is more important in determining vibrational gas temperatures than absorption of quanta) and for optically-thin jets.

Within the bounds of the above-mentioned assumptions the problem splits into two independent parts: joint solution of gasdynamical and relaxational equations and consequent evaluation of the optical properties, which are determined by beforehand calculated distributions of vibrational temperatures and thermodynamic parameters of gases and particles.

It is characteristic for the third stage RE plume that relaxational processes and emissions of the largest part of the molecular vibrational energy at the nozzle exit are terminated before the influence of the ambient stream becomes essential. This influence displays itself by jet compression and penetration of ambient stream molecules inside the RE plume. Therefore, on solving the gasdynamic part of the problem we can limit ourselves to studying continuous flow conditions of a jet spreading into vacuum.

Thus, one has to use system (3) (gasdynamic equations) omitting dissipative terms and adding summands accounting for the change of gas and particle enthalpy due to radiation. Besides, one has to consider nonequilibrium of vibrational degrees of freedom in the gas enthalpy. We should also note that absence of mixing and chemical reactions result in constant mole fractions of gas species along streamlines.

The RE jet outflowing to vacuum is characterized by big turn angles of its gas component. Therefore, during the joint solution of the gasdynamic and relaxation equations we use 'natural' coordinates: a streamline and a normal [13, 14]. In these coordinates the system of the gasdynamic and relaxation equations looks as follows:

$$\frac{\partial}{\partial s}(\rho qr)+\rho qr\frac{\partial}{\partial n}=0,$$
$$\rho q\frac{\partial q}{\partial s}=-\frac{\partial P}{\partial s}-\sum_k\rho_k\left[q_{ks}\frac{\partial q_{ks}}{\partial s}+q_{kn}\frac{\partial q_{ks}}{\partial n}\right.$$
$$\left.-q_{kn}\left(q_{ks}\frac{\partial\theta}{\partial s}+q_{kn}\frac{\partial\theta}{\partial n}\right)\right]$$

$$\rho q^2 \frac{\partial \theta}{\partial s} = -\frac{\partial P}{\partial n} - \sum_k \rho_k \left[q_{ks} \frac{\partial q_{kn}}{\partial s} + q_{kn} \frac{\partial q_{kn}}{\partial n} + q_{ks}\left(q_{ks} \frac{\partial \theta}{\partial s} + q_{kn} \frac{\partial \theta}{\partial n} \right) \right]$$

$$\rho q \frac{\partial H}{\partial s} = -\sum_k \rho_k \left(q_{ks} \frac{\partial H_k}{\partial s} + q_{kn} \frac{\partial H_k}{\partial n} - W \right) - \rho W$$

$$\frac{\partial}{\partial s}(\rho_k q_{ks} r) + \frac{\partial}{\partial n}(\rho_k q_{kn} r) + \rho_k r \left(q_{ks} \frac{\partial \theta}{\partial n} - q_{kn} \frac{\partial \theta}{\partial s} \right) = 0$$

$$q_{ks} \frac{\partial q_{ks}}{\partial s} + q_{kn} \frac{\partial q_{ks}}{\partial n} - q_{kn}\left(q_{ks} \frac{\partial \theta}{\partial s} + q_{kn} \frac{\partial \theta}{\partial n} \right)$$

$$= F_{pk}(q - q_{ks}) q_{ks} \frac{\partial q_{kn}}{\partial s} + q_{kn} \frac{\partial q_{kn}}{\partial n} + q_{ks}\left(q_{ks} \frac{\partial \theta}{\partial s} + q_{kn} \frac{\partial \theta}{\partial n} \right)$$

$$= -F_{pk} q_{kn} q_{ks} \frac{\partial H_k}{\partial s} + q_{kn} \frac{\partial H_k}{\partial n} = -\{\Phi_{pk}(T_k - T_k^*) + F_{pk}[q_{ks}(q_{ks} - q) + q_{kn}^2]\}$$

$$\rho = P \Big/ \left(RT \sum_i C_i \right)$$

$$q \frac{\partial \varepsilon_\alpha}{\partial s} = f_\alpha(c_i, T, P, \varepsilon_\beta). \tag{7}$$

Here $\partial/\partial s$, $\partial/\partial n$ are derivatives along a streamline and its normal, respectively; θ is the angle between the tangent of the streamline and the symmetry axis; q is the gas speed; q_{ks} and q_{kn} are tangent and normal velocities, respectively, of the kth class of particles; W and W_k are specific radiation powers of the gas component and the kth particle class, respectively. The relaxation equations are written for the number ε_α of vibrational quanta in every vibrational mode of the gas mixture [15]. The function f_α describes the change of the molecular vibrational energy due to VT-processes (an energy exchange between vibrational degrees of freedom and translational and rotational degrees), VV'-processes (a vibrational energy exchange between different types of vibrations) and spontaneous emission of quanta.

We consider the plume composition to include the following species: N_2, CO_2, CO, H_2O, H_2, HCl and NO. For such mixture the basic VT-processes are [16]:

$$N + M_i \rightleftarrows N_2 + M_i,$$

$$CO_2(v_2) + M_i \rightleftarrows CO_2 + M_i,$$

$$CO^* + M_i \rightleftarrows CO + M_i,$$

$$H_2O^*(v_2) + M_i \rightleftarrows H_2O + M_i,$$

$$H_2^* + M_i \rightleftarrows H_2 + M_i,$$

$$HCl^* + M_i \rightleftarrows HCl + M_i,$$

$$NO^* + M_i \rightleftarrows NO + M_i,$$

with * designating a vibrationally-excited molecule, M_i standing for a molecule of the i-th species.

The fastest among VV'-processes are vibrational energy exchanges between the modes characterized by the least variation of total vibrational energy. For the plume gas mixture these processes are [16–18]:

$$CO_2(001) + M_i \rightleftarrows \begin{bmatrix} CO_2(110) + M_i \\ CO_2(030) + M_i \end{bmatrix}$$

$$CO_2(100) + M_i \rightleftarrows CO_2(020) + M_i$$

$$H_2O(100) + M_i \rightleftarrows H_2O(020) + M_i$$

$$H_2O(001) + M_i \rightleftarrows H_2O(020) + M_i$$

$$H_2O(100) + M_i \rightleftarrows H_2O(001) + M_i$$

$$N_2^* + CO_2(000) \rightleftarrows N_2 + CO_2(001)$$

$$CO^* + CO_2(000) \rightleftarrows CO + CO_2(001)$$

$$N_2^* + CO \rightleftarrows N_2 + CO^*$$

$$N_2^* + NO \rightleftarrows N_2 + NO^*$$

$$CO^* + NO \rightleftarrows CO + NO^*$$

$$CO_2(001) + NO \rightleftarrows CO_2 + NO^*.$$

The relaxation equations are written in harmonic oscillator approximations with the assumption being made that the Boltsmann distribution is valid for every mode [15]. Rate constants of vibrational relaxation processes have been taken from papers [16–19].

During the joint numerical solution of gasdynamic and relaxation equations a marching method has been used. Integration of 'stiff' relaxation equations has been executed as a separate stage, during which all gasdynamic parameters in a tube of flow were considered constant for a step, and for a number vibrational quanta (ε_α) in every vibrational mode an analytical solution has been written [20, 21]. The exponential behavior of the solution prevented a 'swing' of the system and provide the stable solution for every step.

Distributions of gasdynamic parameters and temperatures of vibrational modes have been determined as a result of calculations. Also, fields of densities and temperatures of solid and liquid particles have been evaluated.

MECHANISMS OF PLUME EMISSIONS IN DIFFERENT SPECTRAL RANGES

During the development of calculation methods of the plume radiation characteristics we divided a large amount of the processes and mechanisms responsible for the plume emissions into few main groups. We suppose that in the model involved it is possible to first calculate gasdynamical flowfields and then use them to evaluate radiation characteristics.

In general when calculating plume emission characteristics one should consider not only absorption and emission processes, but also the light scattering on the condensed-phase particles: Al_2O_3 and soot. The

appropriate integro-differential transfer equation can be represented in the symbolic form:

$$\frac{dI_\nu}{dx} = -K_\nu I_\nu + A_\nu \tag{8}$$

where I_ν is a spectral radiance, K_ν is an attenuation coefficient, A_ν is a source function (which is also known as an emission coefficient). For two-phase media one should take into consideration gas and particle contribution in the attenuation coefficient and the source function. It is possible to represent the coefficient in the following form:

$$K_\nu = k_{\nu\,\mathrm{gas}} + k_{\nu\,\mathrm{abs}} + k_{\nu\,\mathrm{scat}} \tag{9}$$

where $k_{\nu\,\mathrm{gas}}$ is a gas-phase absorption coefficient, $k_{\nu\,\mathrm{abs}}$ and $k_{\nu\,\mathrm{scat}}$ are absorption and scattering coefficients of the condensed phase, respectively.

As the characteristic temperature at the exhaust of the plume engine varies in the range of 1500 K–2000 K the basic mechanism of the own plume emission is a thermal one in the i.r. spectral range (1–6 mkm) and it is caused by radiation of the vibration–rotational (VR) bands of exhaust molecular components (first of all H_2O, CO, CO_2 and HCl) and of the condensed-phase (Al_2O_3 and soot) particles. As we already noted, at high altitudes one should consider a nonequilibrium character of the radiation in VR bands.

First of all we will review methods calculating a gas-component radiation. In the case of a local thermodynamic equilibrium (LTE) the 'gas' part ($A_{\nu\,\mathrm{gas}}$) of the source function describing thermal radiation of plume gases is evaluated by the Plank function ($B_\nu(t)$) and the absorption coefficient ($k_{\nu\,\mathrm{gas}}$):

$$A_{\nu\,\mathrm{gas}} = k_{\nu\,\mathrm{gas}} B_\nu(T). \tag{10}$$

Due to a sharp spectral and temperature dependence of the absorption coefficient within the VR bands, when calculating selective radiation of the gas component and its passing through the atmosphere one should use specific models of molecular VR bands, choose appropriate methods accounting for spacial inhomogeneity of the path and analyze the validity of initial spectral information. The methods for calculating the plume optical features in the VR bands are based on the works Refs. [22–24].

At high altitudes a rapid plume expansion results in violation of the LTE conditions and a difference between vibrational and translational temperatures of molecular gas bands appears. In this case the calculation methods should explicitly consider populations of the upper vibrational levels. In general, it amounts to the following, as we have to calculate the radiance averaged over some frequency interval ($\Delta\nu \sim 10\ \mathrm{cm}^{-1}$)

$$I_\nu = \frac{1}{\Delta\nu}\int_{\nu-\Delta\nu/2}^{\nu+\Delta\nu/2} I_{\nu'}\,d\nu' \tag{11}$$

it is appropriate to use the band model developed in the work [25]. The lines of several different vibrational transitions get into the averaging interval. For each vibrational transition the lines getting into the certain interval are approximately situated on equal distances from each other and line strengths slowly vary in the interval; therefore, the Elsasser model can be applied to describe them. Due to inharmonism and vibration–rotation interaction the locations of the lines belonging to different vibrational transitions are not correlated and it is possible to use the statistic model to account for their overlapping.

Within the bounds of the assumptions involved the equation of transfer for a nonuniform path can be written in the following form:

$$\bar{I}(\nu)|_{x=R} = \int_0^R \left(\Sigma B_k \frac{d\ln\tau_k}{dx}\right)\tau\,dx. \tag{12}$$

Here $B_k(\nu)$ is an extension of the Plank function on nonequilibrium conditions [11]. According to the statistic model the slab transmissivity τ or overlapping of different transitions can be expressed as follows:

$$\tau = \prod_k \tau_k, \tag{13}$$

where τ_k is a transmissivity for the lines belonging to the same transition in the Elsasser approximation.

The problem of calculating an unselective component of the plume emission amounts to the account of radiation and scattering on Al_2O_3 and soot particles. The contribution of the particles ($A_{\nu\,\mathrm{part}}$) to the source function can be given in the following form:

$$A_{\nu\,\mathrm{part}} = k_{\nu\,\mathrm{scat}}\int_\Omega (I(\Theta) + I_{\mathrm{ext}}(\Theta)) \times p(\cos\Theta)\,d\Omega/4\pi + A_{\nu\,\mathrm{own}} \tag{14}$$

where $p(\cos\Theta)$ is a phase function, Θ is a scattering angle, I_{ext} is an external radiance incident to the plume (the Sun and engine nozzle radiation), $A_{\nu\,\mathrm{own}}$ is an own condensed-phase radiation coefficient. The first term in system (14) describes the scattering of the own plume and external radiations in condensed-phase particles (we integrate by the solid angle); the second term is the own particle radiation.

The Al_2O_3 and soot particles of RE plumes form a polydisperse medium, i.e. they are continuously distributed by their sizes. The optical characteristics of an elementary volume of the disperse medium ($k_{\nu\,\mathrm{scat}}$, $k_{\nu\,\mathrm{abs}}$, $p(\cos\Theta)$, $A_{\nu\,\mathrm{own}}$) are evaluated by the averaging of the appropriate individual particle characteristics over a particle size distribution. During gas-dynamic flowfield calculations of the solid RE plume, the size distribution of polydisperse Al_2O_3 particles is simulated by few particle groups; each group is considered to consist of particles of the same size. To calculate the disperse phase radiation one should previously evaluate density and temperature fields and phase states of each particle group. The development of methods calculating elementary volume charac-

teristics ($k_{v\,scat}, k_{v\,abs}, p(\cos\Theta)$ and $A_{v\,own}$) is a distinct problem in this case.

To strictly account for the scattering on the condensed-phase particles one should solve the complicated integro-differential equation of transfer (8). The solution of this equation for the nonuniform plume containing a selectively emitting gas component is an impossible problem to solve. In practice different approximate methods are applied. In particular, for the real disperse particle composition in RE plumes it is possible to apply the approach based on the 'big particles' approximation. For such particles the scattering basically goes forward, i.e. the dispersion index has a sharp asymmetric form. In this case we can simulate the basic index petal by the δ-function, i.e. using the so-called 'transport' approximation [26]. In general, such an approach permits one to separate 'gas' and 'dispersible' parts of the plume emission during calculations and simplify evaluation of both own and scattered plume radiation.

In the simplest case the radiance for a nonuniform path in the condensed phase cloud is represented by the formula:

$$\bar{I}_{k,v} = \sum_i \frac{\pi R_i^2 N_i}{\Delta v} \int_{v-\Delta v/2}^{v+\Delta v/2} dv \int_0^R dx k_{abs}^i B_v(T_i). \quad (15)$$

We consider that the absorption efficiency factor $k_{abs}^i \sim n_2$, where n_2 is the Al_2O_3 absorption coefficient (the imaginary part of the complex factor of dispersion), with $n_2 \ll 1$. Therefore, $k_{abs}^i \ll 1$ and the cloud can be considered to be 'optically thin' with respect to absorption.

Using evaluated flowfields of gasdynamic parameters, vibrational temperatures of gases and condensed-phase particles it is possible to find both the emission in the vibrational–rotational bands of molecular gases and the radiation of the condensed particle cloud. The above-stated model results in the following scheme calculating the radiation at the frequency v along the observation path [28]. The nonuniform slab is divided into N uniform zones. For each zone all thermodynamic parameters are given. The radiation is evaluated by the formula:

$$\bar{I}_v = \sum_{n=1}^{N} B_v(n)[\tau_v(n-1) - \tau_v(n)], \quad \tau_v(0) = 1. \quad (16)$$

The values of the effective Plank function $B_v(n)$ and transmissivity

$$\tau_v(n) = \prod_k \tau_{v,k}(n)$$

are determined by the contribution of all vibrational transitions, which lines get into the frequency interval $v \pm \Delta v/2$. From zone to zone the transmissivity and the effective Plank function vary as follows:

$$\tau_{v,k}(n) = \tau_{v,k}(n-1) - D[\tau_{v,k}(n)] \quad (17)$$

$$B_v(n) = \frac{\sum_k B_v(n) D[\tau_{v,k}(n)]}{\sum_k D[\tau_{v,k}(n)]} \quad (18)$$

The value $D[\tau_{v,k}(n)]$ in the Elsasser approximation is evaluated as:

$$D[\tau_{v,k}(n)] = \int_{-d/2}^{d/2} dv \exp\left[-\sum_i^{n-1} \omega_i F_{k,i}(v)\right] \times [1 - \exp(-\omega_n F_{k,n}(v))] \quad (19)$$

where d is the distance between lines, ω_n is the effective thickness of the nth zone, $F_{k,n}(v)$ is the Elsasser absorption coefficient. Thus, the calculation amounts to the sequential item-by-item examination of vibrational transitions. For every transition we evaluate the mean distance between lines, the mean square of their matrix elements and populations of the upper and lower levels. For each zone the sums

$$\sum_k B_v(n) D[\tau_{v,k}(n)], \quad \sum_k D[\tau_{v,k}(n)]$$

and the product

$$\prod_k \tau_{v,k}(n)$$

are accumulated. The procedure is continued until further transitions fail to significantly contribute to the values accumulated.

The calculation of the condensed-phase radiance amounts to the evaluation of the integral (15), where the only undetermined variable is the absorption efficiency factor k_{abs}^i, which can be evaluated from the optical characteristics of the substance by Mie theory methods [27].

Ultraviolet and visible radiations

The ultraviolet and visible radiations are determined by elementary emission processes and depend upon the temperature, pressure and concentrations of emitting components. Radiation mechanisms will be considered for jets at altitudes of 0–50 km. In general, at these altitudes exhaust products afterburn. This results in increasing of the plume temperature and a sharp growth of radical concentrations. The emission in spectral ranges mentioned is due to electron transitions in atoms and molecules, whose excitation takes place at sufficiently large temperatures. The characteristic temperature of the afterburning jet (~ 2000 K) is considerably lower than the characteristic temperature of the electron level excitation ($\sim 10\,000$ K). Therefore, along with thermal excitation of these levels (basically due to collisions with few rapid molecules, which thermal velocities correspond to the temperature of $\sim 10\,000$ K), chemical excitation reactions gain a special significance. For example, the energy released in radical recombination reactions excites an electron level of one of the reactants and then is emitted as a quantum of radiation. In after-

burning plumes, reaction rates and concentrations of radicals involved are sufficiently high. In many cases this results in chemiluminescent radiation exceeding the thermal one.

When the Sun illuminates the plume, photo-excitation of atom and molecule electron states can take place at high altitudes. At low altitudes the influence of these processes is not considerable with respect to chemical and collisional excitations; but when the pressure decreases (at higher altitudes) and the afterburning gradually ceases (the chemical excitation lowers too) then the influence of these processes increases. However, at these altitudes the Sun radiation scattered on plume particles prevails as a rule. In this article we will limit ourselves by considering the own plume radiation in the u.v. and visible spectral ranges.

The basic molecular components of an RE jet are H_2, CO, H_2O, CO_2 and N_2. Mole fractions of these gases are about 0.1–0.3 at the nozzle exit. The solid fuel RE contains the HCl and Al_2O_3 particles having mole fractions of approximately 0.1. Mole fractions of other nitrogen species can have values of 10^{-3} or less. Jets of hydrocarbon fuel REs additionally contain C_2, CH, CH_4, other hydrocarbon molecules and soot particles having mass fractions about 0.001. The metallized fuels lead to the appearance of different metal species (first of all K, Na, Li, Fe, etc.). Thus, possible emitters in the visible and u.v. spectral ranges can be some tens of atoms, molecules and particles. In general, this makes the problem quite boundless. Therefore, one should choose basic radiation mechanisms for a particular composition at the nozzle exit.

Evaluation of thermal radiation levels for the molecular band systems and atom lines in the spectral ranges involved have been performed for two afterburning jets. One simulates a solid fuel RE, the other a liquid one. We have considered the following molecular band systems: the O_2 Schuman–Runge, the OH violet, β, γ, δ and ε bands of NO, the CO Fourth Positive, and N_2 Second Positive, other band systems of H_2, H_2O, CO_2 and N_2. The K, Na and Li resonance doublets are also included. The comparison of these evaluations with calculations of the chemiluminescent (HL) reaction radiations have shown that the basic mechanisms of the gas-phase emission are the latter. In particular, radical recombination results in excitation of the OH violet system ($^2\Sigma - {}^2\Pi_{1/2,3/2}$) and K and Na resonance lines. The recombination reactions CO + O and NO + O give intensive continuous radiation in the visible and the nearest u.v. spectral ranges.

The chemical mechanism of OH Violet system excitation includes two reactions [28, 29] activating several vibrational levels of the $^2\Sigma^-$ electron state:

$$H + OH + OH \rightarrow H_2O + OH^*(^2\Sigma^-, v' = 0, 1, 2, 3), \quad \text{(I)}$$

$$O + H \rightarrow OH^*(^2\Sigma^-, v' = 2) \quad \text{(II)}$$

and two reactions of collisional and radiative quenching of the state [30, 31]:

$$OH^* \rightarrow OH + h\nu, \quad \text{(III)}$$

$$OH^* + M_i \rightarrow OH + M_i, \quad \text{(IV)}$$

The concentration of excited hydroxyl is determined with the widely used assumption about local equilibrium of the hemiluminescent mechanism (I)–(IV):

$$[OH^*]_{v'} = \frac{k_I^{v'}[OH]^2[H]}{\sum_i k_{IV}^i [M_i]}, \quad v' = 0, 1, 2, 3,$$

where $[OH^*]_{v'}$ is the number of excited OH molecules ($^2\Sigma^-, v'$) per m^3; $k_I^{v'}$ is the rate of the (I) reaction; k_{IV}^i is the rate of the (IV) reaction for different molecules M_i; square brackets embracing a chemical formula of a molecular mean a number of appropriate molecules per m^3. In the denominator of this formula we omitted the term responsible for radiative quenching of excited hydroxyl. Estimates show that at pressures about 1 atm the collisional quenching considerably exceeds the radiative one. When the pressure lowers, the excitation reactions get decelerated (as a cube of the pressure for the (I) reaction and as a square for the (II) reaction) together with reactions of collisional quenching (as a square of the pressure). Therefore, the influence of radiative quenching increases. Nevertheless, for pressures exceeding 0.01 atm we can omit the radiative quenching. For $v' = 2$ one should add the summand $k_{II}[O][H]$ to the numerator of this formula. The summand considers the influence of the (II) reaction.

We evaluated radiation of the excited hydroxyl using of the absorption coefficient smoothed over its rotational structure [10, 32]. The emission coefficient smoothed over its rotational structure too is evaluated by the same way as the absorption coefficient [32] and looks as follows:

$$J_\lambda = \frac{16\pi^3 hc}{3g'_e} \frac{10^{30}}{\Delta\lambda} \int_{\lambda-\Delta\lambda/2}^{\lambda+\Delta\lambda/2} \frac{d\lambda'}{\lambda'^6} \sum_{v'v} \frac{q_{v'v} S_e(\lambda_{v'v})}{kT_r} \frac{[OH^*]_{v'} B_{v'}}{|B_{v'} - B_v|} \cdot$$

$$\exp\left[- \frac{hcB_{v'}}{kT_r(B_{v'} - B_v)} \left(\frac{10^6}{\lambda'} - \frac{10^6}{\lambda_{v'v}} + B_v \right) \right] \frac{W}{m^3 \cdot sr \cdot \mu m} \quad (20)$$

where J_λ is the emission coefficient averaged over the interval $\Delta\lambda = 0.005$ μm, $q_{v'v}$ is the Frank–Condon factor, S_e is the square of the matrix element of the molecule dipole momentum (atomic units), T_r is the rotational temperature [K] of the upper electron state, $B_{v'}$ and B_v are the rotational constants [m^{-1}] of the upper and lower states, respectively. We sum up over the bands, which initial wave lengths $\lambda_{v'v}$ (μm) satisfy the inequality:

$$\left(\frac{10^6}{\lambda'} - \frac{10^6}{\lambda_{v'v}} + B_v\right)\frac{1}{(B_{v'} - B_v)} > 0. \qquad (21)$$

The basic assumption in deriving of equation (20) is overlapping of the OH rotational lines that does not take place at temperatures about 2000 K observed at afterburning jets. In this case one of the authors [33] compared thermal radiation of the (0, 0) band of the OH violet system consisting of isolated Doppler lines for a two-slab problem (slab temperatures ranged from 300 to 3000 K and optical thicknesses from 0 to 10^4) with the band radiation calculated with the absorption coefficient averaged over its rotational structure. The maximal difference reaches a factor of three. This is quite acceptable since rates of the excitation reactions (I) and (II) are known with accuracy of up to the order of magnitude.

Initial data for calculating the emission J_λ and absorption K_λ coefficients are spectroscopic constants [34] and probabilities T_{jj} of the vibrational–rotational transitions [35], normalized such a way that the transition probability of the P_1(i) line of the (0, 0) band equals to 1.

Continuous emission of the carbon and nitrogen oxide flames is connected with chemiluminescent reactions [36, 37]:

$$CO + O \rightarrow CO_2 + hv, \qquad (V)$$

$$NO + O \rightarrow NO_2 + hv. \qquad (VI)$$

At the nozzle exit an RE jet contains considerable quantities of CO (mole fractions range from 0.1 to 0.3) and in the afterburning zone mole fractions of atomic oxygen reach 10^{-2}. All this stipulates the significant role of the process (V). The estimate of the contribution of nitrogen species reactions shows that the maximal NO mole fraction is 10^{-3} and the NO_2 mole fraction is 10^{-6}, therefore, a role of the reaction (VI) is smaller than the (V) one, since rates of both reactions are of the same order of magnitude [36, 37].

The spectral distributions of the CO + O reaction radiation spread from 0.30 to 0.70 μm with maximum at 0.45 μm; while the reaction (VI) radiation occupies the spectral range from 0.4 to 1.4 μm with maximum about 0.65 μm. The emission coefficients for these sources are

$$J_{\lambda CO-O} = \frac{hc}{4\pi\lambda} k_V [CO][O] f_{CO-O}(\lambda), \quad \frac{W}{cm^3 \cdot sr \cdot \mu m}$$

$$J_{\lambda,NO-O} = \frac{hc}{4\pi\lambda} k_{VI} [NO][O] f_{NO-O}(\lambda), \quad \frac{W}{cm^3 \cdot sr \cdot \mu m} \qquad (22)$$

where f_{CO-O} and f_{NO-O} (μm^{-1}) are spectral distributions (normalized to 1) of these chemiluminescent reactions [36, 37]. The temperature distortions of these distributions are not large and are not taken into consideration. We calculated radiations of these reactions using the 'volume source' approximation ($K_\lambda = 0$) because the light absorption of the CO_2 molecules is negligible in the visible spectral range (the absorption cross section $\sim 10^{-20}$ cm^2) and the NO_2 mole fraction is very small (not more than 10^{-6}).

In scientific literature there is not a uniform opinion on the mechanism of alkaline metal radiations in afterburning jets. For example, the authors of Ref. [39] have calculated the Na resonance doublet radiation in an afterburning jet at normal pressure evaluating the kinetics of the chemical excitation and quenching of the appropriate atom levels. However, the authors of Ref. [38] have pointed out that at low altitudes the thermal radiation of the alkaline metals exceed the chemiluminescent one.

The mechanism of activating a doublet component of the first excited level of the alkaline metal Me, where Me is potassium, sodium or lithium in the ground state, includes the following radical recombination reactions [39–41]:

$$H + H + Me \rightarrow H_2 + Me^* \qquad (VII)$$

$$H + OH + Me \rightarrow H_2O + Me^* \qquad (VIII)$$

$$O + O + Me \rightarrow O_2 + Me^* \qquad (IX)$$

The energy released in these recombinations excites the $^2P_{3/2}$ or $^2P_{1/2}$ levels of the alkaline metal (Me* means a metal atom in one of these states). The second important source of *Me* excitation is collisions with arbitrary molecules *M* of jet gases

$$Me + M \rightarrow Me^* + M. \qquad (X)$$

The Me* quenching occurs in processes of collisional and radiational deactivation:

$$Me^* + M \rightarrow Me + M \qquad (XI)$$

$$Me^* \rightarrow Me + hv. \qquad (XII)$$

Rates of the reactions (VII–IX) or K and Na are in [40, 41]. Supposing that the number [Me*] of excited Me* atoms per cm^3 is quasistationary for the $^2P_{3/2}$ state we get

$$[Me^*] = \frac{\frac{2}{3}[Me](k_{VII}[H]^2 + k_{VIII}[H][OH] + k_{IX}[O]^2 + k_X[M])}{A + k_{XI}[M]}. \qquad (23)$$

The factor 2/3 is stipulated by the assumption that the reactions (VII–IX) with equal probability populate all sublevels of the $^2P_{3/2}$ or $^2P_{1/2}$ state differing by their momentum projections. For the $^2P_{1/2}$ state this factor equals 1/3. The maximal estimate for the [Me*] is obtained by omitting the *A* term that is the probability of the spontaneous emission (s^{-1}) and is responsible for radiative quenching of excited levels.

The spectral emission coefficient for one of the double lines equals

$$J_\lambda = \frac{[\mathrm{Me}^*]A}{4\pi}\frac{K_\nu}{S}h\nu, \quad \frac{\mathrm{W}}{\mathrm{cm}^3 \cdot \mathrm{sr} \cdot \mathrm{cm}^{-1}} \tag{24}$$

Here K_ν is the spectral absorption coefficient [cm^{-1}], S is the line strength [cm^{-2}]. This formula has been written in the assumption that shapes of emission and absorption lines coincide and that the radiation is isotropic. Hence, we get the equation for the line center frequency ν_0:

$$\frac{J_{\nu 0}}{K_{\nu 0}}S = \frac{[\mathrm{Me}^*]A}{4\pi}h\nu_0 \tag{25}$$

which we have used to evaluate radiation transfer in the isolated line of the alkaline metal. We calculated the radiation of the K lines (0.7665 and 0.7699 μm), Na lines (0.5890 and 0.5896 μm) and Li line (0.6708 μm). For Li both doublet lines merge together because of the smallness of multiplet splitting.

QUALITATIVE STRUCTURE OF THE PLUME RADIATION SPECTRUM

The above-stated analysis of the gasdynamic structure formation and plume radiation processes allows one to obtain qualitative estimates of the radiation spectrum structure and its distortion caused by increasing of the flight altitude. At the i.r. spectrum range the plume radiation is concentrated in shortwave bands of molecular components (basically in the H_2O and CO_2 bands) underlaid by the gray (nonselective) background that is stipulated by the condensed-phase (soot and metal oxides) radiation. The radiant intensity in different spectral ranges is determined by exhaust component concentrations, the plume effective temperature and absorption coefficients of emitting components. At afterburning altitudes, emitting gas concentrations and temperatures depend not so much on the nozzle exit conditions as on the quantity of unburned products in the exhaust and their interaction with the atmosphere. For this reason a solid fuel RE, which contains relatively high concentrations of H_2 and CO, has higher effective temperatures and therefore, more powerful radiation than a liquid fuel RE with the same mass flow. Also, the maximum of the radiation spectrum lies in the more shortwave range for the first RE. Nevertheless, on the whole, plume radiation spectra have similar qualitative appearances in the i.r. range both for solid and liquid REs.

The radiation in the visible range is basically determined by the condensed-phase particles (soot and metal oxides). For a solid fuel RE, the considerable quantity ($\sim$40%) of the Al_2O_3 particles and higher temperatures in the afterburning zone result in an essentially bigger relative fraction of the radiation in the visible and UV ranges than for a liquid fuel RE. For a liquid fuel RE, in the visible range one can see the chemiluminescent radiation caused by the above-stated mechanisms underlaid by the soot radiation.

When afterburning ceases (at the altitudes higher than 40–50 km) the plume radiation weakly depends on interaction with the atmosphere and is basically determined by the parameters at the nozzle exit. For a solid fuel RE, altitude increasing causes a temperature lag between Al_2O_3 particles and gases. The plume radiation spectrum of the solid fuel RE is mainly formed by hot particles and shortwave bands do not essentially distort the smooth spectrum of their radiation. A growth of the radiant intensity with the flight altitude can be observed. The growth is caused by the reduction of the interaction of hot solid particles with the ambient stream. At altitudes higher than 110 km the whole particles cooling becomes stable and is determined by the radiative luminescence. The luminescence of the gas component is linked with the nearnozzle zone; one should only consider a nonequilibrium character of the shortwave band radiation.

To illustrate the above-stated analysis we have calculated several model jets. The conditions and the nozzle exit (the temperature, velocity, pressure, mole fractions of gas components and mass fraction of the Al_2O_3 particles) and the nozzle radius chosen for the calculation are shown in the Table 2.

The plume radiant intensities or the SFRE (solid fuel RE) are displayed in Figs. 1–3. In the vertical axis there are values of the plume radiant intensity ($\mathrm{W} \cdot \mathrm{sr}^{-1}\ \mu\mathrm{m}^{-1}$), in the horizontal axis there are wavelengths (μm). The above-stated features of the spectrum are distinctly observed on these figures. The H_2O and CO_2 shortwave bands basically contribute to the i.r. range and their relative contribution to the long wave end increases with altitude. When afterburning ceases (at the altitudes higher than 35 km) the basic i.r. radiation is concentrated in the CO_2 band of 4.3 μm. The Al_2O_3 particles radiate in the visible range and the contribution of the visible radiation sharply increases at high altitudes (more than 70 km).

In Figs. 4 and 5 there are plume spectra of the LFRE (liquid fuel RE). Changes with altitude in the i.r. range are similar to that of the SFRE spectrum but they display themselves not so clear.

The distinctive feature of the plume radiation in the

Table 2. Conditions at the nozzle exit plane

Stages	Solid fuel RE 1	2	3	Liquid fuel RE 1	2
T_a [K]	2000	2000	2000	2000	2000
U_a [m s^{-1}]	2500	2500	2500	2500	2500
R_a [m]	0.5	0.5	0.3	0.5	0.5
P_a [atm]	1.0	0.3	0.1	1.0	0.3
H_2	0.3	0.3	0.3	0.05	0.05
H_2O	0.1	0.1	0.1	0.4	0.4
CO	0.3	0.3	0.3	0.05	0.05
CO_2	0.05	0.05	0.05	0.15	0.15
HCl	0.15	0.15	0.15	—	—
N_2	0.1	0.1	0.1	0.35	0.35
Al_2O_3	0.3	0.3	0.3	—	—

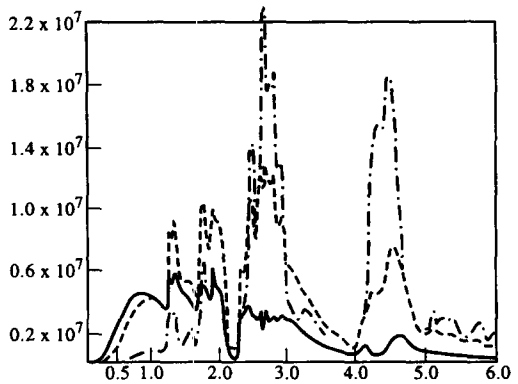

Fig. 1. The spectral radiant intensity of the first stage SFRE plume. The solid line is appropriate to the flight attitude of 10 km, the dashed line 20 km and the dotted line 30 km.

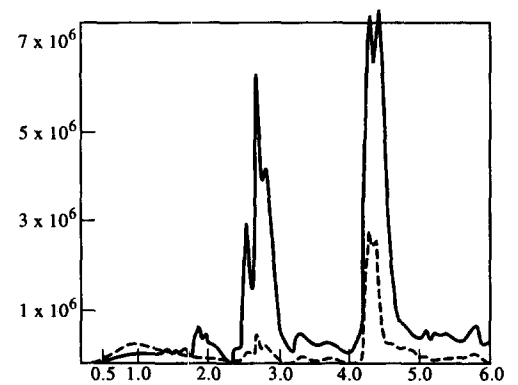

Fig. 2. The spectral radiant intensity of the second stage SFRE plume. The solid line is appropriate to the flight altitude of 35 km, the dashed line 50 km.

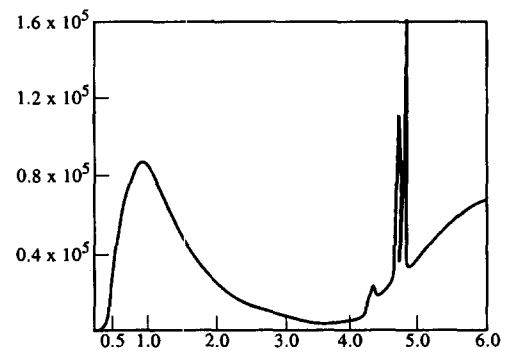

Fig. 3. The spectral radiant intensity of the third stage SFRE plume (expanding to vacuum).

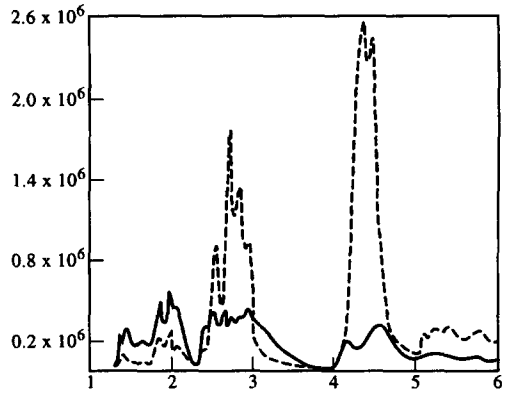

Fig. 4. The spectral radiant intensity of the first stage LFRE plume. The solid line is appropriate to the flight altitude of 10 km, the dashed line 30 km.

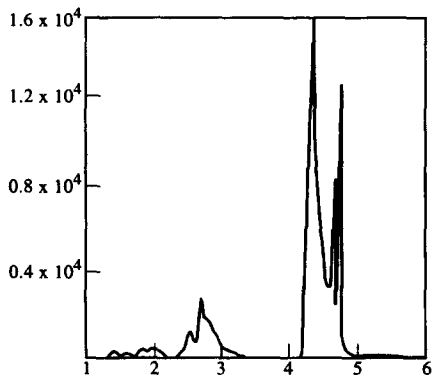

Fig. 5. The spectral radiant intensity of the third stage LFRE plume (expanding to vacuum).

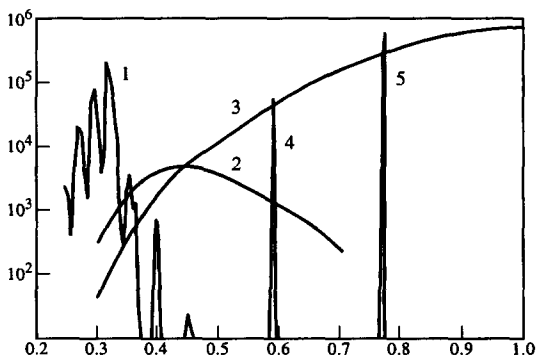

Fig. 6. The radiation spectrum of a typical SFRE plume in the visible and UV ranges at the altitude of 15 km. 1 is the chemiluminescent (HL) radiation of the OH violet bands, 2 the radiation of the CO + O reaction, 3 the thermal radiation of the Al_2O_3 particles and 4 and 5 are HL radiations of the K and Na resonance lines, respectively. The spectral radiant intensity of the Na (and K) resonance doublet is calculated from the integral one by substituting the real doublet shape with the triangular one with a width of 50 Å.

visible and the nearest u.v. ranges is the fact that in spite of its little contribution to the total plume radiant intensity, its role in particular spectral ranges can be essential. It especially concerns to the radiation of the OH violet band system and lines of alkaline metals because molecular bands and atom lines are quite narrow. In Fig. 6 one can find the radiation spectrum of a typical SFRE plume in the visible and u.v. ranges at the altitude of 15 km. This spectrum is calculated with relatively low resolution (~50 Å). On the background of nonselective sources (the thermal radiation of the Al_2O_3 particles and the chemiluminescence radiation of the CO + O reaction) one can distinguish the

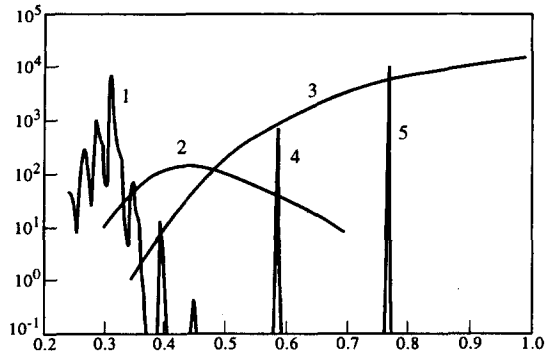

Fig. 7. The radiation spectrum of a typical LFRE plume in the visible and UV ranges at the altitude of 10 km. 1 is the HL radiation of the OH violet bands, 2 the radiation of the CO+O reaction, 3 the thermal soot radiation and 4 and 5 are thermal radiations of the K and Na resonance lines, respectively.

OH violet bands, K and Na resonance lines excited in radical recombination reactions.

In Fig. 7 there is the spectrum of a typical LFRE plume at an altitude of 10 km calculated with high resolution. In this case, nonselective sources are represented by the thermal soot radiation and the CO+O reaction radiation. The relative contribution of the chemiluminescent radiation of the OH violet bands for the LFRE is higher than for the SFRE. It is connected with reducing of the thermal particle radiation because of the lower than for the SFRE temperatures. If we calculate this spectrum with higher resolution ($\sim$1 Å), the shapes of alkaline metal lines become partially separated and the maximum the K and Na resonance line thermal radient intensity can be equal to or higher than the OH bands radiation.

REFERENCES

1. W. W. Dorrance, Viscous hypersonic flow, in *Theory of Reacting and Hypersonic Boundary Layers* McGraw–Hill, New York (1962).
2. *Handbook of Turbulence. Vol.* 1. *Fundamentals and Applications* (Edited by W. Frost and T. H. Moulden). Plenum Press, New York, (1977).
3. H. S. Pergament and H. F. Calcote, Thermal and hemiionization processes in afterburning rocket exhausts, in *11th Int. Symp. on Combustion*, Combustion Inst., Pittsburgh, PA, pp. 597 (1967).
4. V. K. Baev, V. N. Golovichov, P. K. Tretyakov *et al.*, *Combustion in a Supersonic Stream*. Nauka, Novosybirsk (1984).
5. D. E. Jensen and H. S. Pergament, Effects of nonequilibrium chemistry on electrical properties of solid propellant rocket exhaust plumes, *Combust. Flame* **17,** 115–124 (1971).
6. L. S. Evans and C. J. Schexnayder, Influence of chemical kinetics and unmixedness on burning in supersonic hydrogen flames, *AIAA J.* **18,** 188–193 (1980).
7. A. S. Suprun, Programmed preprocessor for chemical kinetics, *Kinet. Catal.* **33,** (1992).
8. D. J. Carlson, R. F. Hogland, Particle drag and heat transfer in rocket nozzles, *AIAA J.* **2,** 1980–1984 (1964).
9. C. B. Henderson, Effect of crystallization kinetics on rocket performance, *AIAA J.* **15,** 600–602 (1977).
10. V. A. Kamenschikov, Y. A. Plastinin, V. M. Nilolayev and L. A. Novitsky, *Radiation Properties of Gases at High Temperatures*. Mashinostroenie, Moscow (1971).
11. V. I. Kruglov and Yu. V. Khodyko, Vibrational nonequilibrium radiation in diatomic gases—Part 1, 2, *Int. J. Heat Mass Transfer* **21,** 163–173 (1978).
12. L. V. Katkovsky, V. I. Kruglov and Yu. V. Khodyko, Method of Markov chains simulation in incoherent radiation transfer theory, *Acta Phys. Polon.* **B11,** 707–715 (1980).
13. F. P. Boyton and A. Thompson, Numerical computation of steady, supersonic, two-dimensional gas flow in natural coordinates, *J. Comput. Phys.* **3,** 379–398 (1969).
14. C. F. Checkmarev and P. A. Skovorodko, Marching method for computation of supersonic viscous gas flow in natural coordinates. Preprint of IT SO AN SSSR: N 71–81, Novosybirsk (1981).
15. A. S. Birukov, Kinetics of physical processes in gas dynamic lasers, *Trudy FIAN* **83,** 13–86 (1975).
16. E. A. Ashratov and N. V. Dubinskaya, Investigation of nozzle flows with vibrational relaxation, in *Computational Methods and Programming*, pp. 96–115. Moscow (1977).
17. B. F. Gordiets, A. I. Osipov and L. A. Shelepin, *Kinetical Processes in Gases and Molecular Lasers*. Nauka, Moscow (1980).
18. S. A. Losev, *Gas Dynamic Lasers*. Nauka, Moscow (1977).
19. V. N. Makarov and S. A. Losev, About influence of impurities on optical amplification coefficient of relaxing gas flow in supersonic nozzles, *Fiz. Gor. Wzryva* **11,** 804–807 (1975).
20. F. G. Blotter, Finite difference methods of solution of boundary layer equations, *AIAA J.* **8,** 193–199 (1970).
21. E. I. Vitkin, A. V. Eremin, V. S. Zibirov, A. A. Kirillov and L. T. Perelman, Investigation of nonequilibrium processes arising at starting of underexpanded jet, Part 1. Preprint of Institute of Physics, Belarus Academy of Sciences, N 570, Minsk (1989).
22. S. S. Penner, *Quantitative Molecular Spectroscopy and Gas Emissivities*. Addison–Wesley, Reading, MA (1959).
23. R. M. Goody, *Atmospheric Radiation*. Oxford University Press, Oxford (1964).
24. C. L. Tien, *Thermal Radiation Properties of Gases, Advances in Heat Transfer*, pp. 253–324. Academic Press, New York (1968).
25. E. I. Vitkin, S. L. Shyralev and V. V. Tamanovitch, Method of computing radiation transfer of vibration–rotation bands of nonequilibrium gases along nonuniform paths. Preprint of Institute of Physics, Belarus Academy of Sciences, N 459, Minsk (1987).
26. K. S. Adzerikho, *Lectures on Radiation Transfer Theory*. Izd-vo BGU, Minsk (1975).
27. H. C. Van de Hulst, *Light Scattering by Small Particles*. Wiley, New York (1957).
28. W. E. Kaskan, Abnormal excitation of hydroxyl in $H_2/O_2/N_2$ flames, *J. Chem. Phys.* **31,** 944–956 (1959).
29. H. G. Wolfhard and E. Hink, Elementary processes in low pressure flames and their relation to rocket plume radiation, *11th Int. Symp. on Combustion*, Combustion Institute, Pittsburgh, PA (1967).
30. H. P. Hooymayers and C. Th. J. Alkemade, Quenching of excited hydroxyl ($^2\Sigma^+, v' = 0$) in flames, *JQSRT* **7,** 495–504 (1967).
31. T. Carrington, Electronic quenching of OH($^2\Sigma^+$) in flames and its significance in the interpretations of rotational relaxation, *J. Chem. Phys.* **30,** 1087–1095 (1959).
32. *Optical Properties of Hot Air* (Edited by L. M. Biberman). Nauka, Moscow (1970).
33. A. S. Suprun, An approximate method of calculation of diatomic molecule UV-radiation at low pressures, *Inz. Fiz. Z.* **51,** 51–57 (1986).
34. *Thermodynamic Properties of Individual Substances*

(Edited by V. P. Glushko), Vol. 1, Moscow, Izd. AN SSSR (1962).
35. J. Anketell and R. C. M. Learner, Vibration rotation interaction in OH and the transition moment, *Proc. R. Soc. Lond.* **A301,** 355–361 (1967).
36. W. G. Browne, D. R. White and G. R. Smokler, *12th Int. Symp. on Combustion*, Pittsburgh, PA (1969).
37. A. Fontijn, C. B. Meyer and H. I. Shiff, Absolute quantum yield measurements of the NO−O reaction and its use as a standard for chemiluminescent reactions, *J. Chem. Phys.* **40,** 64 (1964).
38. D. E. Jensen, D. B. Spaulding, D. G. Tatchell and A. S. Wilson, Computation of flames with recirculating flow and radial pressure gradients, *Combust. Flame* **34,** 309 (1979).
39. R. B. Lions, J. Wormhoudt and C. E. Kolb, Calculation of visible radiation from missiles, *AIAA 16th Thermophysics Conf.* AIAA paper N 81-1111, 23–25 June, Palo Alto, CA.
40. R. Carabetta, W. E. Kaskan, Hemiexcitatin of sodium in flames, *11th Int. Sympo. on Combustion*, Combustion Institute, Pittsburgh, PA, p. 321 (1967).
41. T. M. Sugden, Excited species in flames, *A. Rev. Phys. Chem.* **13,** 369–390 (1962).